Large-Scale Uniform α-$Co(OH)_2$ Long Nanowire Arrays Grown on Graphite as Pseudocapacitor Electrodes

Jian Jiang,[†] Jinping Liu,[†] Ruimin Ding,[†] Jianhui Zhu,[†] Yuanyuan Li,[‡] Anzheng Hu,[†] Xin Li,[†] and Xintang Huang*,[†]

Institute of Nanoscience and Nanotechnology, Department of Physics, Huazhong Normal University, Wuhan 430079, P. R. China, and Department of Electronic Science and Technology, Huazhong University of Science and Technology, Wuhan 430074, P.R. China

ABSTRACT Large-scale uniform α-$Co(OH)_2$ nanowire arrays (NWAs) with an average length of ~20 μm grown on pyrolytic graphite (PG) were successfully synthesized by a hydrothermal method at 120 °C. Ultrasonication test was carried out toward the as-made nanoarray products and the result demonstrated their robust adhesion to graphitic substrate. After 300 s of sonication testing, α-$Co(OH)_2$ NWAs could still possess both integrated one-dimensional (1D) nanoarray architecture and good electronic connections with current collector. When investigated as electrochemical pseudocapacitor electrodes, α-$Co(OH)_2$ NWAs exhibited good energy-storage performance in terms of high specific capacitance of 642.5 F/g, good rate capability, and excellent capacity retention. Our work not only presents a cost-effective and scale-up synthetic method for α-$Co(OH)_2$ NWAs but also holds promise in general synthesis of long arrays of other metal hydroxides/oxide (TiO_2, Fe_2O_3, SnO_2, etc.) nanostructures on PG substrate by using α-$Co(OH)_2$ NWAs as sacrificial templates.

KEYWORDS: α-$Co(OH)_2$ • long nanowire arrays • robust adhesion • graphite substrate • supercapacitor • sacrificial template

INTRODUCTION

As a most promising energy conversion/storage and power output technology for digital communications and hybrid electronic vehicles, electrochemical capacitors have attracted much interest because of their advantages of high power delivery and excellent cycling lifespan in comparison to batteries (1−4). The capacitance of traditional electrical double-layer capacitors (EDLCs) originates from the sole charge separation process occurring at the electrode/electrolyte interface (5). However, such a limited specific capacitance of EDLCs is far from perfect in accordance with the ever-growing need for peak-power assistance in electric vehicles. In contrast, electrochemical pseudocapacitors (using hydroxides, oxides and conductive polymers, etc.) exhibit much higher specific capacitance and energy density due to their reversible multielectron redox Faradaic reactions (6−8). The performance of electrochemical materials is influenced by numerous factors, such as specific surface area, particle size, morphology, Faradaic processes, etc. (9, 10). Particularly noteworthy is the electron transfer between active materials and electrode; establishment of a good electron transport channel to current collector is considered as the fundamental prerequisite for the development of advanced electrochemical devices (11−13).

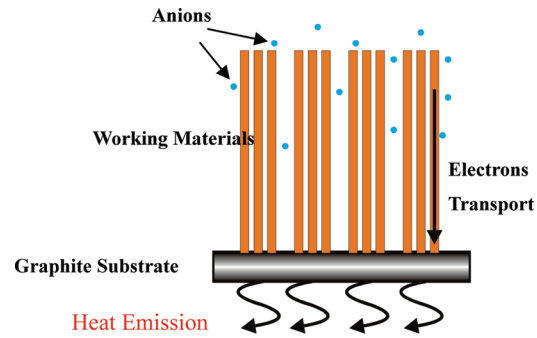

FIGURE 1. Schematic diagram of application advantages of building 1D nanostructured arrays on graphite substrate.

Recently, one-dimensional (1D) nanostructured arrays (14−16) built on conductive substrates have been studied and demonstrated to be an optimized architecture for boosting the electrochemical behaviors of working electrodes (17, 18). As reported single nanowire/nanorod directly contacting with current collector can serve as a superhighway for the fast electron transportation (19, 20). Graphite is a kind of fundamental lightweight material and commonly used as an important component of commercial electrodes due to its low cost, good thermal/electronic conductivity (21) and excellent chemical stability in various electrolytes. Also, single-crystal graphite consisting of numerous graphene sheets stacked together is remarkably useful to synthesize graphene (22−24). Thus, growing inorganic nanowire/rod arrays on economic pyrolytic graphite (PG) substrate (Figure 1) possesses following electrochemical application advantages: (I) the establishment of integrated 1D nanoarray structure renders numerous fast electron-transport accesses

* To whom correspondence should be addressed: Fax +86-027-67861185. E-mail: xthuang@phy.ccnu.edu.cn.
Received for review October 13, 2010 and accepted December 3, 2010
† Huazhong Normal University.
‡ Huazhong University of Science and Technology.
DOI: 10.1021/am1009887

to current collector; (II) well-ordered arrayed architecture is able to reduce the ionic diffusion to the inner part of electrodes, improving utilization of active materials and (III) outstanding thermal conductivity of graphite can facilitate the release of jouleheat yielded from equipment when electrodes are suffering from large discharge currents. To date, some groups have reported the synthesis of simple particle films on bulky PG by chemical vapor deposition (CVD) or layer-by-layer growth method, etc. (25−27). However, to the best of our knowledge, no attention has been yet focused on the direct synthesis of inorganic nanoarrays on PG using a facile solution-based method.

Among transition-metal hydroxides, α-$Co(OH)_2$ has long been investigated as a significant category of electrochemical material and widely used as supercapacitor material because of its high theoretical specific capacitance up to 3460 F/g (28). In this work, we report for the first time a facile and direct synthesis of large-scale α-$Co(OH)_2$ nanowire arrays (NWAs) on PG with a mean length of ∼20 μm via a hydrothermal method. In addition, a sonication test lasting for 300 s toward the nanoarrayed products demostrates their good mechanical adhesion to PG substrate. After sonication test, α-$Co(OH)_2$ NWAs on PG used as electrochemical pseudocapacitors have shown great potential in energy-storage devices and exhibited a high capacitance up to 642.5 F/g, good rate capability and excellent capacity retention. Meanwhile, we also find that scalable growth of α-$Co(OH)_2$ NWAs can be realized regardless of the size or shape of introduced PG substrate.

EXPERIMENTAL SECTION

Synthesis of α-$Co(OH)_2$ NWAs Arrays on PG. PG substrates were obtained from disused batteries (Toshiba Co., Ltd.; AA). In a typical synthesis, 0.582 g (2 mmol) $Co(NO_3)_2 \cdot 6H_2O$, 0.37 g (10 mmol) NH_4F and 0.6 g (10 mmol) $CO(NH_2)_2$ were dissolved in 50 mL of water under magnetic stirring. After 10 min, the as-obtained homogeneous solution was transferred into Teflon-lined stainless steel autoclave and hereafter a piece of clean PG substrate (50 × 7 × 3 mm^3, pretreated by hydrochloric acid (37%) and distilled water successively and dried in air at room temperature) was immersed into the reaction solution, placed against the liner wall, and fixed in the autoclave. Then, the liner was sealed and maintained still at 120 °C for 6 h in an electric oven. After the equipment cooled to room temperature naturally, the PG substrate with pink samples grown on was fetched out and cleaned by an ultrasonication treatment for 20−30 s in order to remove the residual nanoparticle debris.

Characterization Techniques and Electrochemical Testing. For further characterizations and measurements, products on PG substrate were preserved at 300 K in drying oven and then thoroughly characterized with X-ray powder diffraction (XRD, Cu Kα radiation; $\lambda = 1.5418$ Å), scanning electron microscopy (SEM, JSM-6700F; 5 kV) and transmission electron microscopy (TEM and HRTEM, JEM-2010FEF; 200 kV). Electrochemical measurements were conducted in 2 M aqueous KOH (by a half-cell setup configuration) at room temperature on a CHI660C electrochemical working station. A platinum gauze electrode and a standard calomel electrode (SCE) served as counter electrode and reference electrode, respectively. Different from the traditional method (29), after cleanness and encapsulation (in detail, nail enamel was used to insulate the edge of PG.) the products can be directly used as working electrodes; no other ancillary materials such as carbon black or binder were needed.

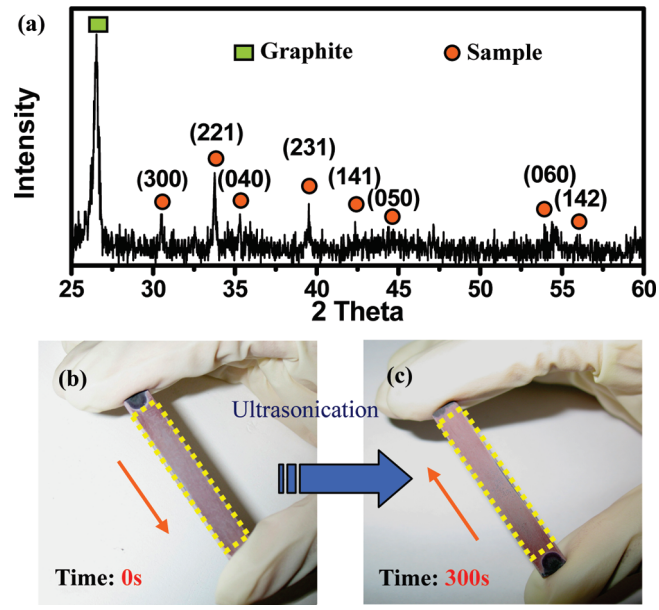

FIGURE 2. (a) XRD pattern of as-made sample grown on graphite. Optical images of α-$Co(OH)_2$ NWAs (b) before and (c) after ultrasonication lasting 300 s.

The mass calculation was made according to weight change caused by the removal of α-$Co(OH)_2$ NWAs via a hydrochloric acid treatment. Each electrode had a geometric surface area of ∼2 cm^2 and contained ∼2 mg of electroactive materials. Capacitances were measured by chronopotentionmetry in a potential range of −0.1−0.45 V and calculated by $I\Delta t/(\Delta V m)$, where I is the constant discharge current, Δt is the discharging time, m is the total mass of the electrode, and V is the voltage drop upon discharging (excluding the IR drop). Examination of mechanical adhesion between nanoarrays and substrate was carried out by using a commercial sonication equipment (power, 250 W; frequencies, 40 K Hz; medium, 50 mL of distilled water) for 300 s.

RESULTS AND DISCUSSION

Figure 2a shows XRD pattern of α-$Co(OH)_2$ NWAs on PG. Obviously, except for a representative peak from PG all the other diffraction peaks can be indexed to cobalt carbonate hydroxide hydrate (CCHH), which is consistent with the value in the standard card (JCPDS Card No.38−0547). Images b and c in Figure 2 respectively display the optical images of the as-made sample before and after ultrasonication testing. As is known, making a good contact between inorganic nanoarrays and substrate is of quite important on electrochemical applications in terms of high-rate electron-transfer devices (18, 19). It is observed that the film of α-$Co(OH)_2$ NWAs can still survive on PG substrate even suffering from a powerful sonication treatment lasting 300 s, from which we can conclude that instead of a precipitation film formed by simple chemical deposition, as-prepared α-$Co(OH)_2$ NWAs with good adhesion property are really grown on graphite substrate. In addition, it is noteworthy that the growth of α-$Co(OH)_2$ NWAs on PG can be achieved regardless of tailored size or shape of graphite substrates. This feature magnifies their potential capability for mass production on large area. To understand the good mechanical adhesion, we believe that defects existing on carbonaceous surface, as recently reported by Dai et al. (29) could

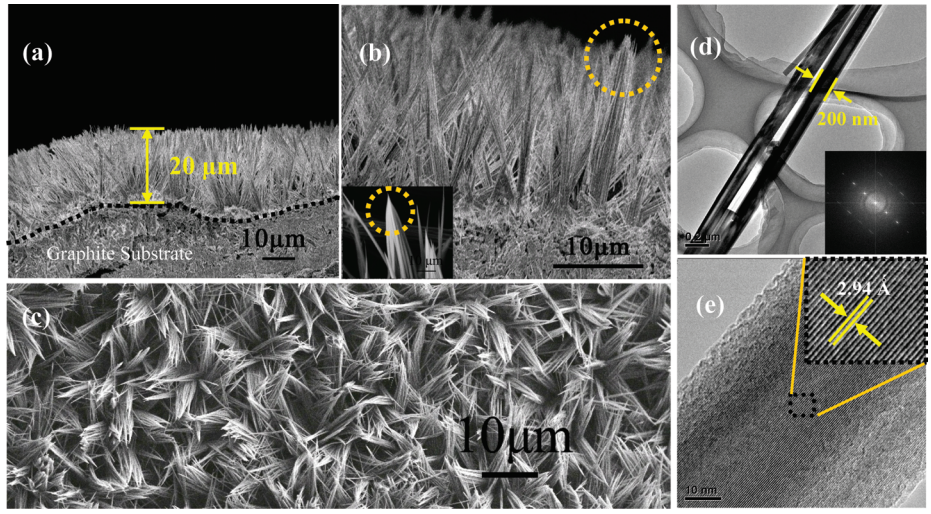

FIGURE 3. (a, b) Cross-sectional and (c) top-view SEM images of α-$Co(OH)_2$ NWAs grown on graphite substrate. (d) TEM image and FFT pattern (inset), and (d) HRTEM image of a single CCHH nanowire.

be very helpful for the growth of hydroxide and formation of strong chemical interactions. Besides, the surface of bulky PG could be oxidized in air atmosphere so that a couple of oxygen functional groups, such as hydroxyl and carbonyl groups, may exist on PG's outer surface (30). These dangling functional groups can act as anchor sites through hydrogen bonding in reaction solution and make the as-formed crystal seeds stick to PG substrate (31).

After sonication testing, α-$Co(OH)_2$ NWAs were in depth characterized by SEM and TEM/HRTEM, respectively. Figure 3a displays the cross-sectional SEM image of uniform α-$Co(OH)_2$ NWAs on PG substrate, from which it is confirmed that the average thickness of α-$Co(OH)_2$ film is of ~20 μm (the dash line represents the interface between arrayed nanowires and PG substrate). Herein, we need to emphasize that among the previous reports (32−34), the length of α-$Co(OH)_2$ nanowire is only around several micrometers (<10 μm). In contrast, the length of α-$Co(OH)_2$ nanowire presented in our work is the longest. Figure 3b shows an enlarged SEM image of Figure 3a. It is interesting to find that several nanowires of α-$Co(OH)_2$ grown nearly vertically to substrate have formed a bundlelike structure on top. Typical top-view SEM image over large area has been made and shown in Figure 3c, which signifies the large-scale growth of α-$Co(OH)_2$ nanostructured arrays on PG substrate. From TEM observation and the fast Fourier transform (FFT) pattern manifested in Figure 3d, we can learn that a single α-$Co(OH)_2$ nanowire with a mean diameter of ~200 nm reveals a high crystallinity property. To make a further investigation on crystallinity, HRTEM observation of a single nanowire has been made. As shown in Figure 3e, the α-$Co(OH)_2$ nanowire exhibits a single-crystalline structure; the spacing of the lattice fringes observed from the magnification region is calculated to be 2.94 Å, which can be indexed as (300) of orthorhombic CCHH.

α-$Co(OH)_2$ NWAs with robust adhesion to conductive graphite electrode were investigated as pseudocapacitors. The interest in studying their electrochemical performances stems from not only the outstanding theoretical capacitance of α-$Co(OH)_2$ but also good electronic connects and nanoarrayed structural features. Thanks to the unique 1D architecture firmly built on current collector, α-$Co(OH)_2$ NWAs can directly serve as working electrodes in the absence of any extra conducting materials or polymer/binder. Figure 4a shows the cyclic voltammetry (CV) curves of α-$Co(OH)_2$ NWAs (on PG) and PG substrate alone in 2 M KOH solution at a scanning rate of 50 mV/s, respectively. According to the literature (28), there are two plausible reactions (quasi-reversible redox processes) occurring at the electrode/electrolyte interface as listed below

$$Co(OH)_2 + OH^- \rightleftarrows CoOOH + H_2O + e^- \quad E_{1/2} = 0.1\ V$$

$$CoOOH + OH^- \rightleftarrows CoO_2 + H_2O + e^- \quad E_{1/2} = 0.4\ V$$

The CV curve of α-$Co(OH)_2$ NWAs is plotted (red), and we can observe that two reversible electron-transfer processes are visible in Figure 4a. This result is consistent with the reaction processes mentioned above during the potential sweep of α-$Co(OH)_2$ NWA electrode, indicating that the measured capacitance is on the basis of the redox mechanism. The CV curve made from PG alone (black) under the same conditions demonstrates that PG electrode itself has an excellent electrochemical stability in alkaline solution within the potential range of −0.3 to 0.6 V (vs SCE) and meanwhile suggests that PG's contribution (double-layer capacitance) to the total electrochemical capacitance can be negligible in contrast with that of α-$Co(OH)_2$ NWAs. Accordingly, we can make a conclusion that α-$Co(OH)_2$ NWAs are totally responsible for the measured capacitance. Figure 4b shows the galvanostatic charge/discharge curve of α-$Co(OH)_2$ NWAs at a current denstity of 1 A/g. The specific capacitance is calculated as high as 642.5 F/g, multiple times higher than that of carbon materials. This is primarily determined by the energy-storage mechanism (36). Although carbon nanotube (CNT) array with high density and long length (~cm) feature

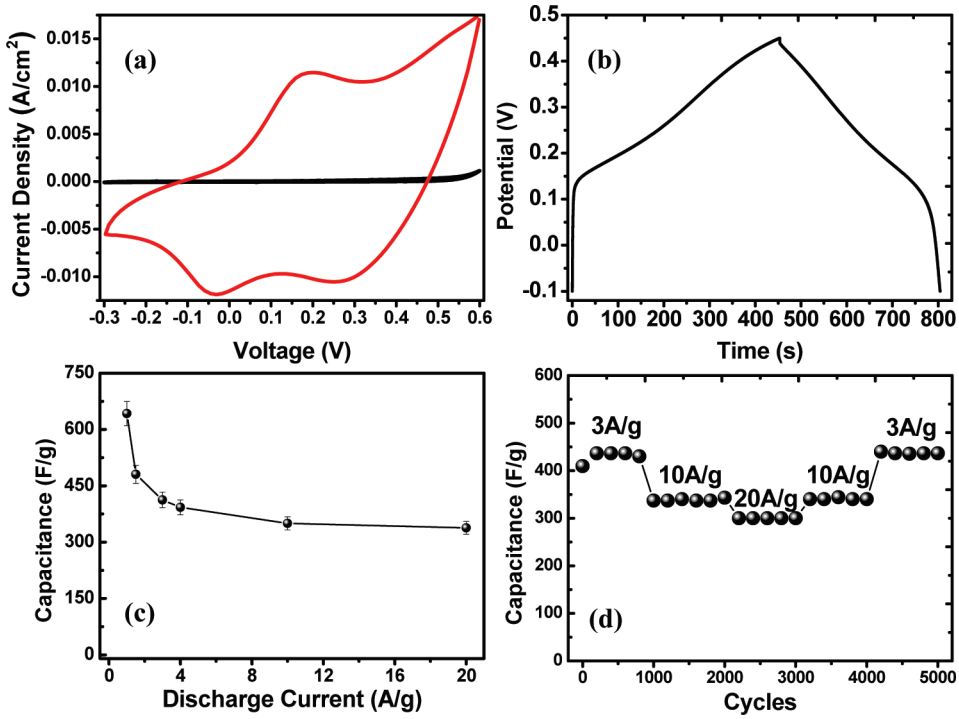

FIGURE 4. (a) CV curves of α-Co(OH)$_2$ NWAs (red) and graphite (black) in potential range of −0.3 to 0.6 V, respectively. (b) Galvanostatic charge−discharge curve, (c) specific capacity (as a function of current density), and (d) cycling performance of as-made sample.

grown on carbon materials (like carbon paper) using CVD method is a kind of promising material for supercapacitors, its specific capacitance value (usually less than 250 F/g) is still limited by the charge storage mechanism of EDLCs, whose capacitances merely depend on the accessible surface area of materials (36, 37), rather than the battery-like reversible faradic reactions; In addition, geometrical and structural advantages of CNT array can only optimize electrochemical performances (rate capability, etc.). Electrochemical capacitances of as-made sample at various discharge current densities have been evaluated and displayed in Figure 4c. With the increasing of discharge current densities, the specific capacitance of α-Co(OH)$_2$ NWAs is calculated to be 480.45 F/g (1.5 A/g), 422.36 F/g (3 A/g), 350.54 F/g (10 A/g), 330.75 F/g (20 A/g), respectively. To the best of our knowledge, the rate performance of α-Co(OH)$_2$ NWAs is far better than that of NiO NWAs (35). From the perspective of engineering/technology and practical working demands, the study in terms of variable power delivery is highly desired and worthy. As can be seen, Figure 4d illustrates the cycling performance of α-Co(OH)$_2$ NWAs on PG with various current densities. The cycling response with a steplike shape at progressive rates can be evidently recorded. Together with the increasing of discharging current rates, the average capacitance of α-Co(OH)$_2$ NWAs can be measured around 430 F/g (3A/g), 345 F/g (10 A/g), and 300 F/g (20 A/g), respectively. Herein, it is noteworthy that the electrode reveals good electrochemical stability even when suffering from sudden change of current delivery. After 3000 cycles, the average capacitance is successively recorded as 340 F/g, 436 F/g by decreasing the current rate from 20 A/g to 3 A/g. Compared with initial cycles, there is no obvious capacitance decrease appearing over 3000 cycles. Besides, the capacitance of α-Co(OH)$_2$ NWAs can be totally recovered after variable power delivery tests. To account for the reasons corresponding to their good electrochemical behaviors, we consider that good capacity retention could be potentially associated with both the robust adhesion between nano materials and PG substrate and the architectural advantages of α-Co(OH)$_2$ NWAs. 1D architecture design provides numerous fast electron-transport accesses to current collector, allowing for quick electron transfer from active redox sites to electrode. On the other hand, large surface to volume ratio of 1D nanostructure is also able to provide more active sites than bulk counterparts and obviously shorten the pathway of anion transport. Furthermore, as a fundamental requirement for free-standing films, good mechanical adhesion plays a key role in ensuring the excellent electrical contact and capacity retention during energy storage/conversion processes occurred in alkaline solution.

Building long functional metal hydroxide/oxide NWAs on conductive substrate is exceptionally important for many applications on energy conversion/storage (e.g., dye-sensitized solar cells and batteries) because long nanowires can elevate the load of active materials, increase the internal surface area, and create more reactive sites (38, 39). However, it remains challenging to synthesize long metal hydroxide/oxide NWAs directly on substrate via simple solution-based method without any seeded process. In our work, there is a highlight that the length of α-Co(OH)$_2$ NWAs is up to ∼20 μm, nearly multiple times that of other metal hydroxides/oxides NWAs (e.g., four times that of ZnO NWAs (∼4 μm)) (40). Recently, Liu et al. reported a novel "sacrificial template-accelerated hydrolysis" (STAH) method for the preparation of FeO_x nanotublar arrays on alloy substrate

using ZnO NWAs as sacrificial templates (17). As a category of hydroxide carbonate, α-$Co(OH)_2$ itself can be gradually dissolved by acid. Accordingly, we suppose that α-$Co(OH)_2$ long NWAs on PG substrate might be capable of being in situ dissolved and serving as sacrificial templates that would in turn initiate nanoarrays formation. This feature shows great potential in the preparation of a wild spectrum of long inorganic oxide NWAs (e.g., NiO, MnO_2, SnO_2, Fe_2O_3, etc.) on PG substrate via "STAH" method. Our future work would focus on this strategy.

CONCLUSIONS

In summary, large-scale α-$Co(OH)_2$ NWAs with a length of $\sim$20 μm has been synthesized on graphite substrate via a hydrothermal method and furthermore applied as electrodes of electrochemical pseudocapacitors. Robust mechanical adhesion of as-made arrayed products is confirmed by a long time sonication test. α-$Co(OH)_2$ NWAs firmly grown on PG save the tedious process of mixing active material with ancillary materials and show a high specific capacitance of $\sim$642.5 F/g, remarkable rate capability, and good capacity retention due to 1D architectural advantages and good electronic contacts. Our result not only presents a cost-effective and scale-up synthetic method for α-$Co(OH)_2$ NWAs but also holds promise in the development of general synthesis of another metal hydroxide/oxide long nanoarrays on PG substrate using α-$Co(OH)_2$ NWAs as sacrificial templates.

Acknowledgment. We gratefully acknowledge financial support from the National Natural Science Foundation of China (50872039 and 50802032), China Postdoctoral Science Foundation (20090460996), the Open Project Program of Key Laboratory of Quak & Lepton Physics (Huazhong Normal University) Ministry of Education, China (QL-PL200902), and the self-determined research funds of CCNU from the colleges' basic research and operation of MOE (CCNU09A01019).

REFERENCES AND NOTES

(1) Service, R. F. *Science* **2006**, *313*, 902.
(2) Bruce, R. F.; Scrosati, B.; Tarascon, J. M. *Angew. Chem., Int. Ed.* **2008**, *47*, 2930–2946.
(3) Talapatra, S.; Kar, S.; Pal, S. K.; Vajtai, R.; Ci, L.; Victor, P.; Shaijumon, M. M.; Kaur, S.; Nalamasu, O.; Ajayan, P. M. *Nat. Nanotechnol.* **2006**, *1*, 112–116.
(4) Miller, J. R.; Simon, P. *Science* **2008**, *321*, 651–651.
(5) Chen, P. C.; Shen, G. Z.; Sukcharoenchoke, S.; Zhou, C. W. *Appl. Phys. Lett.* **2009**, *94*, 043113.
(6) Hu, C. C.; Chang, K. H.; Lin, M. C.; Wu, Y. T. *Nano Lett.* **2006**, *6*, 2690–2695.
(7) Ke, Y. F.; Tsai, Y. S.; Huang, Y. S. *J. Mater. Chem.* **2005**, *15*, 2122–2127.
(8) Xiao, W.; Xia, H.; Fuh, J. Y. H.; Lu, L. *J. Power Sources* **2009**, *193*, 935–938.
(9) Zhou, H. S.; Li, D.; Hibino, M.; Honma, I. *Angew. Chem., Int. Ed.* **2005**, *5*, 807–812.
(10) Hosono, E.; Fujihara, S.; Honma, I.; Ichihara, M. *J. Power Sources* **2006**, *158*, 779–783.
(11) Yu, T.; Zhu, Y. W.; Xu, X. J.; Shen, Z. X.; Chen, P.; Lim, C. T.; Thong, J. T. L.; Sow, C. H. *Adv. Mater.* **2005**, *17*, 1595–1599.
(12) Yu, T.; Zhu, Y. W.; Xu, X. J.; Yeong, K. S.; Shen, Z. X.; Chen, P.; Lim, C. T.; Thong, J. T. L.; Sow, C. H. *Small* **2006**, *2*, 80–84.
(13) Liu, J. P.; Li, Y. Y.; Huang, X. T.; Li, G. Y.; Li, Z. K. *Adv. Funct. Mater.* **2008**, *18*, 1448–1458.
(14) Li, L.; Yang, Y. W.; Li, G. H.; Zhang, L. D. *Small* **2006**, *2*, 548–553.
(15) Ding, R. M.; Liu, J. P.; Jiang, J.; Li, Y. Y.; Hu, Y. Y.; Ji, X. X.; Chi, Q. B.; Wu, F.; Huang, X. T. *Chem. Commun.* **2009**, 4548–4550.
(16) Zeng, H. B.; Xu, X. J.; Bando, Y.; Gautam, U. K.; Zhai, T. Y.; Fang, X. S.; Liu, B. D.; Golberg, D. *Adv. Funct. Mater.* **2009**, *19*, 3165–3172.
(17) Liu, J. P.; Li, Y. Y.; Fan, H. J.; Zhu, Z. H.; Jiang, J.; Ding, R. M.; Hu, Y. Y.; Huang, X. T. *Chem. Mater.* **2010**, *22*, 212–217.
(18) Liu, J. P.; Li, Y. Y.; Huang, X. T.; Ding, R. M.; Hu, Y. Y.; Jiang, J.; Liao, L. *J. Mater. Chem.* **2009**, *19*, 1859–1864.
(19) Jiang, J.; Li, Y. Y.; Liu, J. P.; Huang, X. T. *Nanoscale* **2011**, DOI: 10.1039/c0nr00472c.
(20) Jiang, J.; Liu, J. P.; Ding, R. M.; Ji, X. X.; Hu, Y. Y.; Li, X.; Hu, A. Z.; Wu, F.; Zhu, Z. H.; Huang, X. T. *J. Phys. Chem.C* **2010**, *114*, 929–932.
(21) Taylor, R.; Gilchrist, K. E.; Poston, L. J. *Carbon* **1968**, *6*, 537–544.
(22) Tung, V. C.; Allen, M. J.; Yang, Y.; Kaner, R. B. *Nat. Nanotechnol.* **2009**, *4*, 25–29.
(23) Novoselov, K. S.; Geim, A. K.; Morozov, S. V.; Jiang, D.; Zhang, Y.; Dubonos, S. V.; Grigorieva, I. V.; Firsov, A. A. *Science* **2004**, *306*, 666–669.
(24) Lin, Y. M.; Jenkins, K. A.; Garcia, A. V.; Small, J. P.; Farmer, D. B.; Avouris, P. *Nano Lett.* **2009**, *9*, 422–426.
(25) Yang, H.; Coombs, N.; Sokolova, I.; Ozin, G. A. *J. Mater. Chem.* **1997**, *7*, 1285–1290.
(26) Ma, H. Y.; Hu, N. F.; Rusling, J. F. *Langmuir* **2000**, *16*, 4969–4975.
(27) Li, W. Z.; Wang, D. Z.; Yang, S. X.; Wen, J. G.; Ren, Z. F. *Chem. Phys. Lett.* **2001**, *335*, 141–149.
(28) Cao, L.; Xu, F.; Liang, Y. Y.; Li, H. L. *Adv. Mater.* **2004**, *16*, 1853–1857.
(29) Wang, H. L.; Casalongue, H. S.; Liang, Y. Y.; Dai, H. J. *J. Am. Chem. Soc.* **2010**, *132*, 7472–7477.
(30) Xu, J. J.; Wang, K.; Zu, S. Z.; Han, B. H.; Wei, Z. X. *ACS Nano* **2010**, *4*, 5019–5026.
(31) Wang, Y.; Xia, H.; Lu, L.; Lin, J. Y. *ACS Nano* **2010**, *4*, 1425–1432.
(32) Xu, R.; Zeng, H. C. *J. Phys. Chem. B* **2003**, *107*, 12643–12649.
(33) Hosono, E.; Fujihar, S.; Honma, I.; Zhou, H. S. *J. Mater. Chem.* **2005**, *15*, 1938–1945.
(34) Jiang, J.; Liu, J. P.; Huang, X. T.; Li, Y. Y.; Ding, R. M.; Ji, X. X.; Hu, Y. Y.; Chi, Q. B.; Zhu, Z. H. *Cryst. Growth Des.* **2010**, *10*, 70–75.
(35) Pang, H.; Lu, Q. Y.; Zhang, Y. Z.; Li, Y. C.; Gao, F. *Nanoscale* **2010**, *2*, 920–922.
(36) Zhang, H.; Cao, G. P.; Yang, Y. S. *Energy Environ. Sci.* **2009**, *2*, 932–943.
(37) Kim, B.; Chung, H.; Kim, W. *J. Phys. Chem. C* **2010**, *114*, 15223–15227.
(38) Chan, C. K.; Zhang, X. F.; Cui, Y. *Nano Lett.* **2008**, *8*, 307–309.
(39) Xu, C. K.; Shin, P.; Cao, L. L.; Gao, D. *J. Phys. Chem.C* **2010**, *114*, 125–129.
(40) Liu, J. P.; Huang, X. T.; Li, Y. Y.; Ji, X. X.; Li, Z. K.; He, X.; Sun, F. L. *J. Phys. Chem. C* **2007**, *111*, 4990–4997.

AM1009887